

MODELING THE EFFECTS OF SOLID STATE ORIENTATION ON BLOWN HIGH MOLECULAR WEIGHT HIGH DENSITY POLYETHYLENE FILMS: A COMPOSITE THEORY APPROACH

D. Ryan Breese – Equistar Chemicals, a Lyondell company

Gregory Beaucauge – Department of Chemical and Materials Engineering, University of Cincinnati

Kelly L. Williams – Equistar Chemicals, a Lyondell company

Abstract

High molecular weight high density polyethylenes (HMW-HDPE) are unique, in that they can be uniformly oriented to high draw ratios to produce films with significantly enhanced physical properties. Such improvements are the result of the transformation of isotropic piles of lamellae into rigid, long, fibrous microstructures, which can be characterized by various analytical techniques. This work represents the first industrially usable approach to the prediction of mechanical properties in oriented polyolefin films and may have wider application to other fiber-like microstructure forming polymers. The model presented is tied both to the observed structural features, as well as to properties that are routinely measured in the industrial setting. These enhanced films create new opportunities for flexible packaging in high strength and stiffness applications.

Background

HMW-HDPE films can be oriented to improve physical properties, namely the moduli and tensile yield and break strengths. Several approaches have been proposed to explain the molecular transitions that enhance these properties, but none provide a practical model that correlates with the observed changes in the microstructure of the oriented polymer. To fully understand the structure property relationship of oriented films, any adequate model must incorporate the structural transition that is occurring during the drawing process. Such a model would be beneficial to a fundamental understanding of structure property relationships and for use in polymer development for producing oriented films with improved properties.

The simplest of fiber composites models, the infinitely long [1] and the short fiber composite theories [2, 3] are not used in their basic form to characterize semi-crystalline polymer systems. These models, while simple in nature, do not account for the formation of fibrillar structures that occurs during the orientation process. In addition, to effectively calculate the composite's physical properties, one must know the properties of each component, which are generally unknown for semi-crystalline systems. These simple models do serve as a foundation for building more elaborate theories that closely represent the changes that occur during the drawing of a semi-crystalline polymer.

Peterlin [4] proposed an elaborate structural model that incorporated a hierarchical arrangement of fiber-like

structures. Due to the complexity of this model, no relationships were given that could correlate the enhancements in physical properties to film characteristics. In addition, Peterlin claimed that the improvements in physical properties were solely the result of taut tie molecules in the amorphous phase and could not be correlated to increasing crystalline orientation. Past work [5-8] has shown the changes in film properties can be closely related to the orientation of the crystalline component.

Barham and Arridge [9] and Gibson, Davies and Ward [10] modified the infinitely long fiber composite theory to include a shear lag factor [11] that attempted to account for inefficiencies in the transfer of stress between the matrix to the fiber. The authors' techniques differed in that Barham and Arridge claim the enhancements in properties are the result of the increasing aspect ratio of the fiber, while Gibson, Davies and Ward propose the improved properties are the direct result of an increase in the volume fraction of fibers present in the drawn system. Both sets of authors constructed molecular structures based on anomalies observed in x-ray diffraction data. As a result, the structures they propose do not correlate with structures observed with various microscopy techniques [5, 12-15]. While the structure-property relationships proposed in these models may be misleading, they propose two valuable concepts, the idea of a transition occurring in the crystalline component and the increase in the volume fraction of fibers upon drawing.

Film Fabrication and Orientation

Base films were produced from five different HMW-HDPE grades with typical conditions and techniques on a three layer Hosokawa-Alpine film line. The HMW-HDPEs covered a broad range of densities (0.938 g/cc – 0.959 g/cc) and melt indices (0.05 g/min – 0.10 g/min). The blown film line consisted of three extruders with grooved feed sections and length to diameter ratios of 24:1. The die gap was set at 2000 microns. The films were produced with a stalk height of eight die diameters and a blow up ratio of 4:1. The monolayer base films were 150 microns thick.

The films were oriented off-line on a Hosokawa-Alpine MDO unit. Prior to the drawing stage, the thick film is uniformly preheated to 5-10°C below the polymer's melting temperature. The draw ratio was incrementally increased

from 2:1 to the maximum draw ratio for each polymer, indicated by the breaking of the film. Next, the films were annealed at 5-10°C below the melting temperature. After annealing, the oriented films were then cooled to room temperature by chilled rollers.

Film Characterization

The drawn films were analyzed with various techniques to fully understand how the changes in microstructure relate to the enhancements in physical properties. Optical microscopy (50X magnifications under cross polarizers) and AFM (Atomic Force Microscopy) shows the unoriented film samples have a relatively low degree of orientation on both a large and small length scale, as indicated in Figure 1. Upon orientation, the crystalline region becomes highly oriented in the machine direction on several length scales, as indicated in Figure 2. In addition, fiber-like structures appear to be present in the drawn film, indicating a transition from a relatively randomly oriented crystalline phase to a highly anisotropic crystalline phase that is continuous in the drawing direction. Such a structure has been documented in the literature [5, 12-18].

Several techniques were used to characterize the orientation of the crystalline region of the films. The analysis included wide angle x-ray scattering (WAXS), small angle x-ray scattering (SAXS), birefringence and Fourier Transform optical microscopy.

The WAXS data showed a significant increase in the c-axis orientation of the unit cell upon orientation. At draw ratios greater than 6:1, the orientation of the unit cell was nearly that of a perfectly aligned crystal, with Herman's orientation functions greater than 0.920. This observation indicates a high degree of orientation of the c-axis of the unit cell in the machine direction.

Data collected from SAXS measurements shows the alignment of the lamellae normal in the machine direction at low draw ratios, then the tilting of the lamellae normal to an angle of 34.4° relative to the machine direction. The observed tilt between the lamellae normal and c-axis of the unit cell is inherent to the polyethylene crystal and has been observed by past researchers [19]. Such a structure results in a Herman's orientation function for the lamellae normal of 0.521 at high draw ratios. The onset of this lamellar tilting corresponds with the alignment of the unit cell's c-axis in the machine direction.

Birefringence was utilized to characterize the combined orientation of the amorphous and crystalline phases. An increasing linear relationship was observed between the Herman's orientation function and the draw ratio, as expected from the stress-optical coefficient relationship. Future work is planned to use birefringence in conjunction with crystallographic orientation techniques to characterize the orientation of the amorphous region.

A new technique was used to study the orientation of the crystalline component on a larger length scale by using software to create a Fourier Transform of the optical micrographs. The transformed images were then analyzed with the same code used in the x-ray scattering experiments to determine orientation functions of larger length scale entities. This analysis resulted in a drastic increase in the measured orientation function at moderately high draw ratios, indicating the formation of large length scale fibrous materials at high draw ratios.

A summary of the calculated orientation functions from the various techniques relative to draw ratio is presented in Figure 3.

Modeling an Oriented Semi-Crystalline Polymer Film

Based on the observations through various microscopy and orientation measurements, the infinitely long fiber composite theory was modified to develop a practical model that incorporates the observed transition of crystalline components into fibrous structures.

A three phase composite model was used, which consisted of amorphous, fiber and non-fiber crystalline regimes, as indicated in Equations (1) – (4).

$$E_{C,MD} = E_F V_F + E_{NFC} V_{NFC} + E_A V_A \quad (1)$$

$$E_{C,TD} = \left(\frac{V_F}{E_F} + \frac{V_{NFC}}{E_{NFC}} + \frac{V_A}{E_A} \right)^{-1} \quad (2)$$

$$\sigma_{C,MD} = \sigma_F V_F + \sigma_{NFC} V_{NFC} + \sigma_A V_A \quad (3)$$

$$\varepsilon_{C,MD} = \varepsilon_F \quad (4)$$

Where: $E_{C,MD}$ = composite machine direction modulus
 $E_{C,TD}$ = composite transverse direction modulus
 E_i = modulus of the i^{th} component
 V_i = volume fraction of the i^{th} component
 $\sigma_{C,MD}$ = composite machine direction break strength
 σ_i = machine direction break strength of the i^{th} component
 $\varepsilon_{C,MD}$ = composite machine direction break strain
 ε_i = machine direction break strain of the i^{th} component

In the undrawn film, the non-fiber crystalline phase consists of piles of stacked lamellae [14] with order on short length scales, as seen in Figure 1. Upon orientation, the structure of these lamellae are converted to highly anisotropic fibrillar structures consisting of aligned lamellae stacks, as seen in Figure 2. At this point, it is uncertain whether extended chain structures were formed [13], with future work planned for studying such phenomena.

To simplify the three-phase composite model, contributions from the amorphous region to the overall composite moduli were neglected. This assumption greatly simplifies the model and is justified by the significantly lower moduli of the amorphous phase, relative to that of the crystalline phase,

at the elevated orientation temperature. In addition, from DSC (Differential Scanning Calorimetry) and density column measurements, as well as noted in the literature [12], the percent crystallinity does not change relative to the extent of drawing. This concludes that the amorphous component is not being transformed into fibrillar structures, meaning the percent crystallinity is equivalent to the sum of the percent fibers (V_F) and non-fiber crystalline (V_{NFC}) components.

The lower boundary condition for the model proposes that the volume fraction of fibers in the undrawn film is not necessarily zero, meaning fibrous structures could be present in the undrawn film. Such a condition provides a robust model that can include films produced with various techniques, such as blown (high stalk, in-the-pocket), cast, and sheet. The upper bound limits the percent of fibers to the total percent crystallinity of the undrawn film, indicating that all of the non-fiber crystalline phase has been converted into fiber-like structures at the film's maximum draw ratio. This condition provides a method for determining a realistic fiber modulus. Past authors [9, 10] simply assume the modulus of the fiber component is that of a perfect crystal (~250-300 GPa). Such an assumption results in an unrealistically low volume fraction of fibers, when compared to x-ray and microscopy data.

Substituting the boundary conditions and simultaneously solving the moduli equations for the volume fraction of fibers results in an exponential relationship between the volume fraction of fibers and the characteristic draw ratio (Figure 4), where the characteristic draw ratio is the ratio of the thickness of the undrawn film to the drawn film. In addition, a logarithmic relationship is observed between the modulus of the non-fiber crystalline component and the characteristic draw ratio, a direct result of this phase's transformation into rigid fibrous structures.

When correlating the moduli and break strength to the volume fraction of fibers, linear relationships are evident as indicated in Figures 5-7. The break strain of the composite decreases sharply with the volume fraction of fibers, and beyond a specific volume fraction of fibers, all polymers converge to a common, low break strain (Figure 8). Beyond this critical volume fraction of fibers, the fibrous structures dominate the physical properties of the film, correlating to the break strain indicated in Equation (4).

Conclusions

The work presented describes the first industrially usable technique for predicting enhancements for the design of oriented polyolefin films. This model uses routinely measured film properties to explain how the morphology of the crystalline region of the polymer changes during uniaxial orientation and utilizes practical fiber composite theory to explain how enhancements in physical properties relate to the fiber-like structures present in the film. In addition, this theory could have wider application to other fiber-like microstructure forming semi-crystalline polymers.

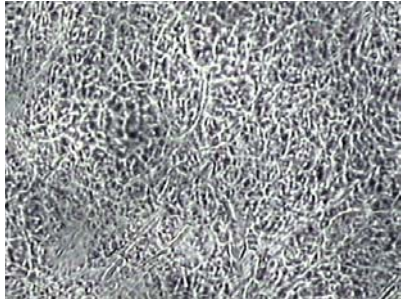
Acknowledgments

The authors would like to thank Dr. Doug McFaddin, Dr. Ayush Bafna, and Dr. Fran Mirabella for their contributions to the analytical characterization of these films. In addition, we would also like to thank Dr. Paul Phillips, Dr. Vassilios Galiatsatos, Dr. Rick Seyler, Dr. Len Cribbs, and Dr. Brad Etherton for their consultation throughout this program. We would also like to thank Mr. David Nunes of Hosokawa-Alpine for granting operating time on their state-of-the-art machine direction orientation (MDO) line. It was truly a pleasure to work with the talented and knowledgeable staff at Hosokawa-Alpine's Augsburg research facility.

References

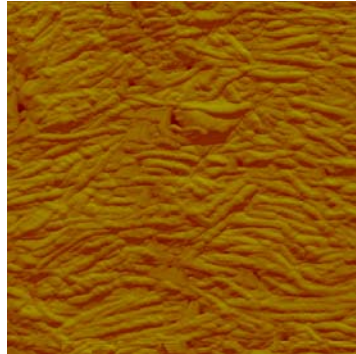
1. Agarwal, B. D., Broutman, L. J., "Analysis and Performance of Fiber Composites" (1990).
2. Ashton, J. E., Halpin, J. C., Petit, P. H., *Primer on Composite Materials Analysis*, (1969).
3. Halpin, J. C., Kardos, J. L., *Journal of Applied Physics*, 45:5 2235 (1972).
4. Peterlin, A., *Advan. Chem. Ser.*, 142:1 (1975).
5. Breese, D. R., Masters Thesis: University of Cincinnati (2004).
6. Gupta, V. B., Keller, A., Ward, I. M., *J. Macromol. Sci.*, B(2):1 139-146 (1968).
7. Crist, Buckley. Annual Review of Materials Science, 25 295 (1995).
8. Zhou, H., Wilkes, G. L., *Journal of Materials Science* 33 287 (1998).
9. Barham, P. J., Arridge, R. G. C., *Journal of Polymer Science, Polymer Physics Edition*, 15 1177 (1977).
10. Gibson, A. G., Davies, G. R., Ward, I. M., *Polymer* 19 683 (1978).
11. Cox, H. L., *British Journal of Applied Physics* 3 72 (1952).
12. Koenig, J. L., Cornell, S. W., Witenhafer, D. E., *Journal of Polymer Science*, A-2:5 301 (1967).
13. Bassett, D. C., Carder, D. R., *Philosophical Magazine*, 28:3 535 (1973).
14. Tagawa, T., *Journal of Polymer Science*, 18 971 (1980).
15. Matsumoto, T., Kawai, T., Maeda, H., *Die Makromolekulare Chemie*, 107 250 (1967).
16. Roe, R. J., Krigbaum, W. R., *J. Chem. Phys.*, 40 2608 (1964).
17. Prasad, A., Shroff, R., Rane, S., Beaucage, G., *Polymer*, 42 3103 (2001).
18. Yu, T-H, Wilkes, G., *Polymer*, 37:21 4675-4687 (1996).
19. Bassett, D. C., Olley, R. H., Al Raheil, I. A. M., *Polymer*, 29 1539 (1988).

**Optical Microscope
50 X Magnification**



165 μm

AFM



2.5 μm

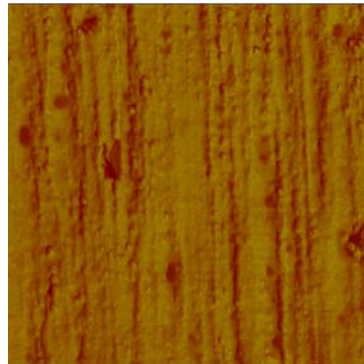
Figure 1. Optical (50X magnification under cross polarizers) and AFM photos of an undrawn film. Machine Direction is vertical.

**Optical Microscope
50 X Magnification**



165 μm

AFM



2.5 μm

Figure 2. Optical (50X magnification under cross polarizers) and AFM photos of film that is highly drawn in the machine direction. Machine Direction is vertical.

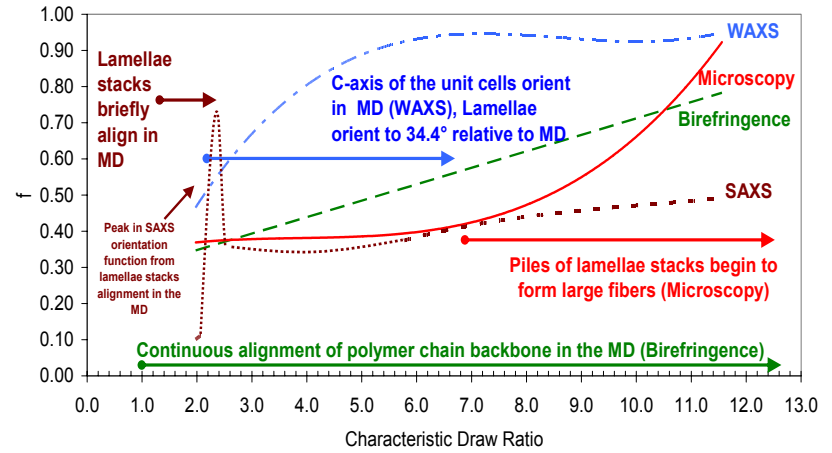


Figure 3. Plot of the orientation functions determined through various techniques vs. characteristic draw ratio.

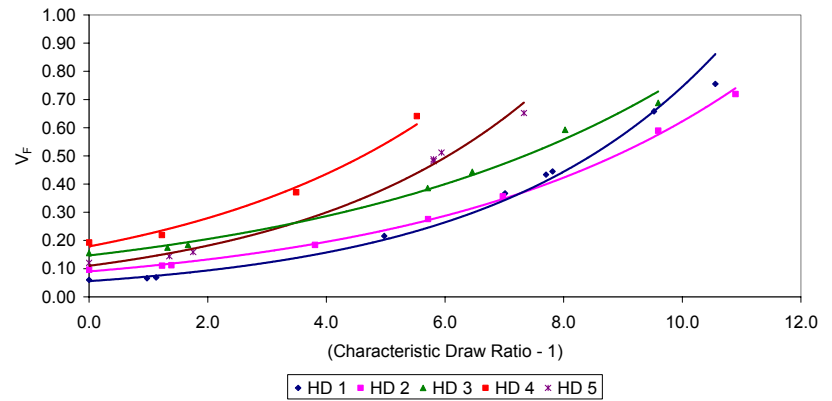


Figure 4. Plot of V_F vs. Characteristic Draw Ratio.

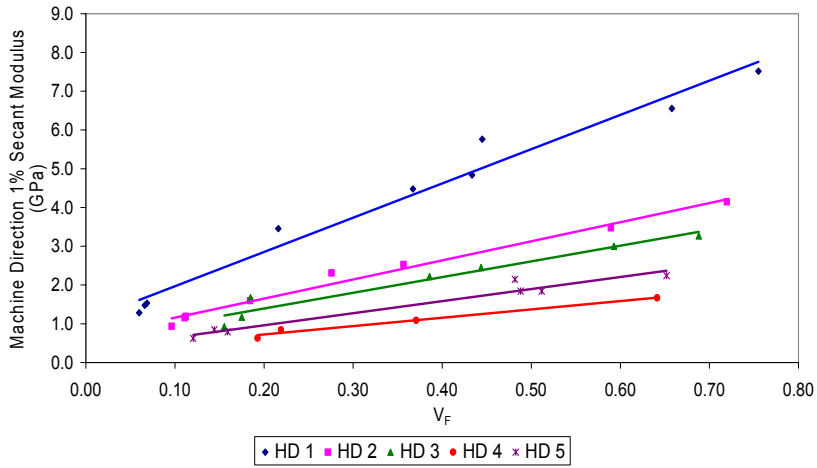


Figure 5. Plot of Machine Direction Modulus vs. V_F .

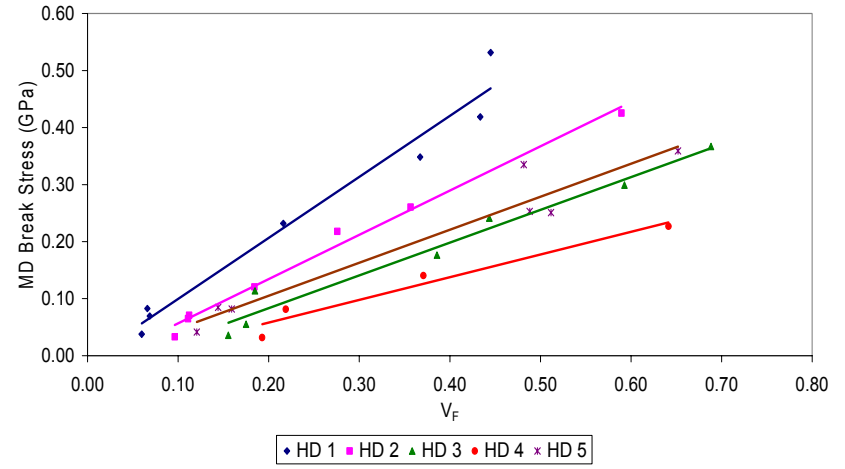


Figure 7. Plot of Machine Direction Break Stress vs. V_F .

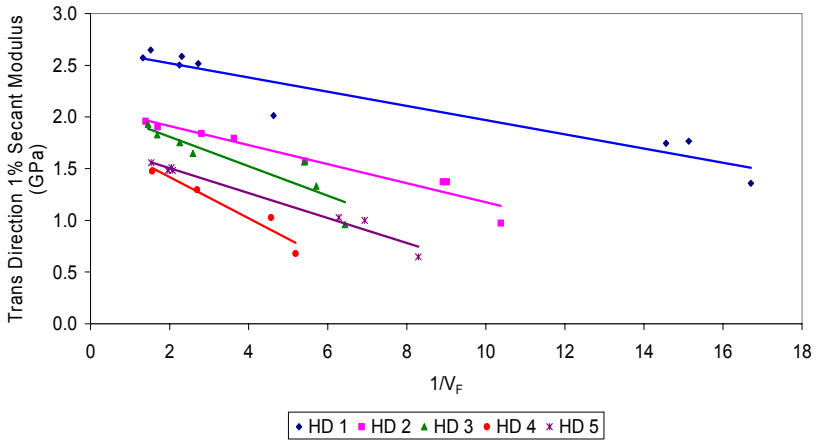


Figure 6. Plot of Transverse Direction Modulus vs. $1/V_F$.

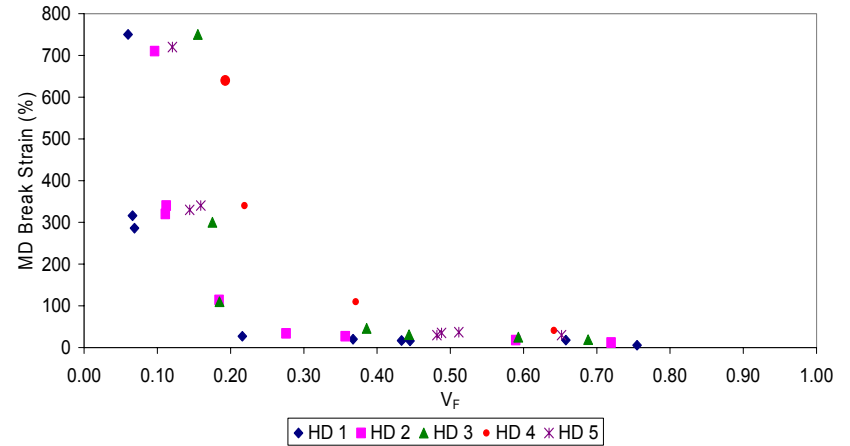


Figure 8. Plot of Machine Direction Break Strain vs. V_F .

Key Words: Orientation, MDO, Polyethylene, Fiber